

Inferring Brown-Capped Rosy-Finch demography and breeding distribution trends from long-term wintering data in New Mexico

New Mexico Department of Game and Fish Share with Wildlife Program

Final Report

June 2025



Brown-capped Rosy-Finch. Photo by Joel Such.

AUTHORS:

Whitney A. Watson, Department of Fish, Wildlife, and Conservation Ecology, New Mexico State University

Corrie C. Borgman, U.S. Fish and Wildlife Service, Division of Migratory Bird Management, Southwest Region

Steven Cox, Rio Grande Bird Research, Inc.

Abby J. Lawson (Principal Investigator), U.S. Geological Survey New Mexico Cooperative Fish and Wildlife Research Unit

ABSTRACT

The three North American Rosy-Finch species (Brown-capped [*Leucosticte australis*], Black [*L. atrata*], and Gray-crowned [*L. tephrocotis*]) are among the most climate-threatened species in the United States. New Mexico is an important location for investigating the effects of climate change because it is the southernmost location in which Brown-capped Rosy-Finches breed and the southernmost location where all three Rosy-Finch species co-occur during winter. In the context of climate change, this range boundary is important to study because it is the first part of the range anticipated to cross a threshold of unsuitability for these species with increasing temperatures. Rosy-Finches are difficult to study during the breeding season due to the high elevation and remoteness of their breeding grounds; therefore, winter studies may lend insight into population trends and provide direction for conservation actions based on knowledge of the breeding origins of wintering birds. The goals of our study were to investigate long-term survival and migration trends from wintering Brown-capped Rosy-Finches in New Mexico and evaluate the efficacy of radio frequency identification (RFID)-equipped artificial feeders to monitor population trends. As of May 2025, we have conducted a robust design survival analysis on 22 years of mark-recapture data from a particular wintering site in New Mexico, assessed patterns in the breeding origins of individuals captured at this site using stable isotope analysis, and examined patterns in data collected via RFID. Our main findings from this study are that annual survival probability of Rosy-Finches wintering in New Mexico is low compared to that of other migratory passerines, that Brown-capped Rosy-Finches wintering in New Mexico likely originate from a variety of locations across their breeding range, and that RFID monitoring is useful in improving survival estimates in Rosy-Finches, particularly in short-term studies.

INTRODUCTION

Rosy-Finches are among the most climate-threatened taxa in the United States. Three species are found in North America: Brown-capped (*Leucosticte australis*; BCRF), Black (*L. atrata*; BLRF), and Gray-crowned Rosy-Finches (*L. tephrocotis*; GCRF); hereafter, the three species will be referred to collectively as Rosy-Finches. Rosy-Finches breed exclusively in tundra or alpine tundra ecosystems and because high elevation regions are predicted to be disproportionately impacted by climate change (Pepin et al. 2015), Rosy-Finches face high risk of habitat loss as a result of tree and shrub encroachment (Grace et al. 2002). Furthermore, changes in insect phenology resulting from climate change may negatively impact food availability and quality. All three species of Rosy-Finch are protected by the Migratory Bird Treaty Act, and BCRF and BLRF are listed as Birds of Conservation Concern by the U.S. Fish and Wildlife Service (USFWS 2021). BCRF and BLRF are also included in the Partners in Flight Red Watch list (Rosenberg et al. 2019) and in seven of eight State Wildlife Action Plans throughout their range, including New Mexico. Despite concern for

these species, little is known about Rosy-Finch life histories, vital rates, and migration patterns.

Although the three North American Rosy-Finch species have distinct breeding ranges (Fig. 1), they occupy a broader range of habitats and may occur in flocks together outside of the breeding season. During winter, Rosy-Finches use a combination of high- and low-elevation areas with varying types and degrees of anthropogenic development and readily approach artificial feeders. Thus, winter field studies offer a valuable opportunity to efficiently acquire demographic data and biological samples for all three Rosy-Finch species with reduced logistical overhead. Our study leverages an existing long-term (22 years) mark-recapture dataset with accompanying feather samples from the Sandia Mountains of New Mexico (Fig. 1) and adds a novel component evaluating the efficacy of radio frequency identification (RFID)-equipped artificial feeders to monitor tagged wintering Rosy-Finches. The Sandia Mountains of central New Mexico is the southernmost wintering locale in which all three Rosy-Finch species co-occur and is the southernmost locale in which any of the three species ever occur (Fig. 1). It is thus a uniquely valuable site to study wintering Rosy-Finch populations and document potential impacts of climate change. Studying peripheral species or populations at or near distributional extents is essential for efficient, long-term conservation planning at landscape scales (Steen and Barrett 2015). Peripheral populations can offer insight into a species' physiological tolerances and their capacity to adapt to climate change (e.g., behavior, physiology, dispersal), which is useful for evaluating the effectiveness of potential management actions to curb or offset predicted environmental changes. We used this long-term mark-recapture dataset to evaluate trends in Rosy-Finch winter survival probability. Among Rosy-Finch studies, this mark-recapture dataset is unique in its longevity, sample size, and location at the southern winter range periphery.

To evaluate the migratory connectivity of Rosy-Finch breeding populations to wintering areas in New Mexico, we conducted hydrogen stable isotope analysis of collected feathers. Hydrogen stable isotope analysis is based on the natural and predictable geographic variation (across latitudinal and altitudinal gradients) in the ratio of hydrogen isotopes (protium [^1H] and deuterium [^2H]) in water molecules, a ratio in the tissues of animals that reflects the geographic location in which the animals grew these tissues. Because Rosy-Finches undergo a complete feather molt on the breeding grounds, analyzing feather tissue collected from birds on their wintering grounds can help identify the areas where the birds were likely to have bred the previous summer (see Task 3 description for more details). Using stable isotope analysis results and available environmental data, we can investigate the influence of climate covariates at breeding areas or wintering sites that may explain variance in the birds' abundance, survival, or inferred breeding origins.

In addition to analyzing the existing mark-recapture dataset, we initiated a pilot study to evaluate the efficacy of RFID-equipped feeders to improve vital rate estimates and evaluate connectivity among wintering sites. Rosy-Finches are known for nomadic behavior during the winter, in which they may make long-range movements within their winter range for reasons that are not well understood. Such movements violate the assumptions of many traditional modeling frameworks; consequently, relatively complex frameworks that require robust sample sizes are needed to provide unbiased vital rate estimates. In recent years, multiple avian studies have demonstrated that equipping grain feeders with RFID-enabled “smart” devices is an effective way to acquire robust visit and movement data from wintering birds that have been marked with tags that the RFID reader can detect at close ranges. This approach was recently used by Latimer and Gardner (2022) in a study on BLRF and GCRF in northern Utah, generating thousands of annual detections to help infer overwinter survival and movement patterns. The RFID component of this study provides a synergistic opportunity to evaluate Rosy-Finch winter movements at small (i.e., within New Mexico) and broad (i.e., across states) scales using the growing network of tagged individuals and RFID-equipped feeders in their wintering range.

Funds from the New Mexico Department of Game and Fish’s Share with Wildlife (SwW) program were used to support three tasks related to BCRF (below), as part of the larger study focused on all three Rosy-Finch species—the focus of Whitney Watson’s PhD dissertation. As such, we report results for all three species for ease of presentation. Similarly, although the SwW funds were only disbursed over calendar years 2023 and 2024 (overlapping with three winter data collection seasons: 2022–2023, 2023–2024, 2024–2025), the funds enabled us to examine two long-term datasets dating back to 2004 (Tasks 1 and 2). Thus, we report results for the entire time period (2004–2025), where relevant. The three tasks are as follows:

Task 1: Demographic analysis of mark-recapture data

Task 2: Stable isotope analysis of feather samples

Task 3: Establish new RFID feeders for the winter (2022–2023 field season)

STUDY AREA

This study was primarily conducted at the highest ridge in the Sandia Mountains of central New Mexico and the southernmost site at which any of the three North American Rosy-Finch species can be found. This site has an elevation of 3,255 m and occurs in the Hudsonian life zone, with forests dominated by Engelmann spruce (*Picea engelmannii*), white fir (*Abies concolor*), and ponderosa pine (*Pinus ponderosa*; Julyan & Stuever 2005). Average temperatures range from -10.5 °C to 5.7 °C and average snow depth ranges from

5.1 cm to 58.4 cm during the months of November–April (Western Regional Climate Center 2025) when Rosy-Finches are typically present in this area.

Additional work for this study was conducted in Taos Ski Valley, New Mexico, another site where Rosy-Finches are consistently found during the winter. This site lies approximately 180 km northeast of the Sandia Mountains site, has an elevation of 2,841 m, and has similar vegetation profile to the Sandia Mountains site. Average temperatures at Taos Ski Valley range from -11.0 °C to 16 °C and average snow depth ranges from 21 cm to 110 cm during November–April.

FIELD METHODS

Rosy-Finches were captured at the Sandia Mountains site each winter from 2004–2025. Captures typically occurred one day per week between the hours of 0600 and 1000 from the month of November to April the following year, with the total number of capture days each winter varying from 6 to 17. Rosy-Finches were captured in a set of mist nets set up in an “L” shape around an artificial bird feeder used as a lure. Upon capture, individuals were banded with a uniquely numbered U.S. Geological Survey (USGS) Bird Banding Laboratory (BBL) aluminum band, identified to species, age class (hatch year or after hatch year), and sex; morphometric measurements (such as mass, fat score, wing chord length, and tail length) recorded. Species, age class, and sex were determined via plumage coloration. Upon recapture of an individual banded on a previous date, the USGS ID was recorded and new morphometric measurements were collected.

Beginning in 2005, the 5th rectrix on the right side of the tail was collected from individuals upon their first capture of the winter season. In winters 2023–2024 and 2024–2025, we collected two rectrices—both the 1st and 5th on the right side of the tail for inter-feather variation study described in Task 3 section below. All feathers were stored individually in paper coin envelopes in a dry, climate-controlled location prior to preparation for stable isotope analysis. From November 2022 to April 2025, captured Rosy-Finches were additionally fitted with a green plastic leg band embedded with a uniquely identifiable 2.6 mm RFID tag (Eccel Technologies, United Kingdom). This study was performed under the auspices of New Mexico State University Institution for Animal Care and Use Committee protocol #2310000718, USGS BBL banding permit #20617, and New Mexico Department of Game and Fish banding permit #1636.

TASK 1: DEMOGRAPHIC ANALYSIS OF MARK-RECAPTURE DATA

Methods

We used a combination of existing (2004–2022) and newly-collected (2022–2025) mark-recapture data (BBL band recapture data only; see field methods above) to evaluate trends in winter survival probability for all three Rosy-Finch species at the Sandia Mountains site. We analyzed the data in a Bayesian robust design framework (Pollock 1982) to estimate annual survival probability (i.e., the probability that an individual in the population survives to the following year and does not permanently emigrate from the study area) for each species. This type of model allows the estimation of survival probabilities for a population using information on detection for a series of secondary sampling occasions within each primary sampling occasion to estimate separate detection probabilities (i.e., the probability that an individual is detected given it is available for detection) within primary sampling occasions and between primary sampling occasions (Kendall et al. 1995, 1997). This in turn allows for estimation of temporary emigration probability (i.e., the probability of an individual being absent from the study area and thus unavailable for capture during a particular primary sampling occasion) and subsequently for the estimation of true survival. This model assumes closure to immigration, emigration, recruitment, and mortality *within* primary sampling occasions, but allows the population to be open to these gains and losses *between* primary sampling occasions.

Following Riecke et al.'s (2018) parameterization of the robust design model, we combined mark-recapture data from all three species into a single model and divided the data within each winter season (our primary sampling occasions) into 11 two-week secondary sampling periods spanning from November 9th of each year to April 11th of the following calendar year. It is reasonable to assume some degree of closure during winter seasons because we don't expect births outside of the breeding season or a large number of deaths outside of migratory periods. We included the main effects of species and age class in addition to an interaction term between species and age on the survival parameter. Because juveniles encountered during mist netting have already survived the post-fledging period and migration to the nonbreeding grounds upon first capture, juvenile survival estimates represent the probability that a hatch-year individual in the population will survive to the next winter, given that it has already survived to its first winter.

We constrained the temporary emigration parameter to be random but constant over time, meaning the probability of an individual being unavailable for detection in a given year was the same across years and does not depend on whether it was unavailable for detection in the previous year. We allowed detection probability to vary with primary sampling occasion and with each two-week secondary sampling period, and fixed

detection probabilities during secondary occasions with no sampling effort to zero. This prevented the model from treating secondary occasions with no sampling effort in the same way as occasions with effort but no detections, which would downwardly bias detection probability. We used zero-mean, normally distributed priors with large variance ($\sigma^2 = 100$) on all parameters except the temporary emigration parameter, for which we used a uniform prior.

We sampled from three Markov chain Monte Carlo (MCMC) chains with 30,000 iterations, a burn-in period of 5,000 and a thinning interval of 10. Adequate mixing of MCMC chains inspected visually via traceplots and $\hat{R} < 1.1$ for all parameters indicated successful model convergence (Brooks & Gelman 1998). All analyses were conducted in program R version 4.4.3 (R Core Team 2025) using the packages *rjags* (Plummer 2024) and *jagsUI* (Kellner 2024).

Results

A total of 3873 unique individual Rosy-Finches were captured over the data collection period of 2004–2025, including 1043 BCRF, 2129 BLRF, and 701 GCRF. There were 8745 total detections during this period including recaptures, of which 5910 were juveniles (hatched during the preceding breeding season), 2793 were adults (hatched prior to the preceding breeding season), and 42 were of unknown age. These individuals of unknown age were removed from the survival analysis, leaving 8703 detections of known-age individuals. Across the data collection period, the mean number of new unique individuals captured and banded per winter season was 48.0 (range 0–293) for BCRF, 97.6 (range 5–578) BLRF, and 32.2 (range 0–188) for GCRF. The mean number of total unique individuals (banded in a previous season or not) was 117.4 (range 0–640) for BCRF, 218.5 (range 8–1039) for BLRF, and 61.7 (range 0–261) for GCRF (Fig. 2).

In our robust design survival analysis, mean annual detection probability for secondary sampling occasions within each winter season ranged from 0.04 to 0.25. The probability that an individual did not temporarily emigrate from the study area was 0.27 (95% credible interval [CrI]: 0.22–0.32). This means 27% of birds present in the study area during a particular winter season are expected to return to the study area the following winter season, suggesting 73% of birds do not show winter site fidelity between consecutive winters.

Survival probabilities were higher in BCRF ($\bar{x} = 0.40$, 95% CrI: 0.31–0.51 for juveniles and $\bar{x} = 0.38$, 95% CrI: 0.32–0.42 for adults) and BLRF ($\bar{x} = 0.27$, 95% CrI: 0.21–0.34 for juveniles and $\bar{x} = 0.41$, 95% CrI: 0.37–0.46 for adults) than in GCRF ($\bar{x} = 0.19$, 95% CrI: 0.11–

0.29 for juveniles and $\bar{x} = 0.24$, 95% CrI: 0.18–0.32 for adults. This is unsurprising because BCRF and BLRF likely migrate shorter distances to the Sandia Mountains site based on the locations of their breeding ranges (Table 1; Fig. 1; Fig. 3). The longer distance that GCRF individuals presumably migrate to reach the Sandia Mountains site from their breeding grounds likely contributes to their lower survival probabilities because migration is generally considered to be the period of highest mortality risk in migratory birds (Holmes 2007; Klaassen et al. 2014; Alerstam & Bäckman 2018). Survival probabilities were higher in adults than juveniles in BLRF and GCRF, but lower in adults than juveniles in BCRF. Lower survival probabilities in adults than juveniles is not typical of migratory passerines (Redmond & Murphy 2012; McKim-Louder et al. 2013), and could be an artifact of sparse data or could indicate a unique pattern of migration among age classes in this particular species. Because juveniles in our study were first captured after they had already survived post-fledging and migration to the nonbreeding (wintering) grounds (likely the periods of highest mortality for juveniles in a population; Gruebler et al. 2014), we do not expect juvenile survival to be as low as if individuals were first marked on breeding grounds.

Our survival estimates for Rosy-Finches are relatively low compared to those for other migratory passerine species (Paxton et al. 2017; Rockwell et al. 2017) and to those of a non-migratory high-elevation specialist, the White-winged Snowfinch (*Montifringilla nivalis*; $\bar{x} = 0.44$ –0.54 for adult males and $\bar{x} = 0.51$ –0.64 for adult females; (Strinella et al. 2020)), which could be indicative of ongoing population declines in these species. Many survival studies, including those cited above, estimate apparent annual survival rates, which are the product of true survival and site fidelity probabilities, and thus are already likely downwardly biased (Lebreton et al. 1992; Schaub & Royle 2014). This implies that our survival estimates are even lower than expected for these species; unfortunately, we lack information on historic Rosy-Finch demographic parameter estimates and estimates for other regions that we could compare with our estimates.

Table 1. Annual survival probability estimates and 95% credible intervals for each of two age classes (juvenile and adult) in each of the three rosy-finch species (brown-capped [“BCRF”], black [“BLRF”], and gray-crowned [“GCRF”]) 2004–2024 from Bayesian robust design survival analysis. β coefficients are given along with back-transformed survival estimates, lower 95% credible interval limits (“LCL”) and upper 95% credible interval limits (“UCL”).

	<i>Juveniles</i>				<i>Adults</i>			
	β	Survival estimate	LCL	UCL	β	Survival estimate	LCL	UCL
BCRF	-0.42	0.40	0.31	0.51	-0.51	0.38	0.32	0.43
BLRF	-1.00	0.27	0.21	0.34	-0.36	0.41	0.37	0.46
GCRF	-1.51	0.19	0.11	0.29	-1.14	0.24	0.18	0.32

Further plans to refine our robust design model include exploring the effects of adding individual sex and body condition covariates on the survival parameter, allowing survival to vary with year, and allowing temporary emigration rates to vary with species and age. We also plan to incorporate a Markovian temporary emigration structure into the model, such that the probability that an individual is available for detection during a particular primary sampling occasion depends on whether it was available for detection during the previous primary occasion. This model structure may better suit Rosy-Finch life history, because many migratory passerines demonstrate some degree of winter site fidelity across years (Somershoe et al. 2009; Pakanen et al. 2018). We also intend to explore an open robust design model (Kendall & Bjorkland 2001), which relaxes the assumption of population closure within the primary sampling occasion and enables the estimation of abundance. This may better reflect the facultative, weather-driven movement of Rosy-Finches during the nonbreeding season (Johnson et al. 2000; MacDougall-Shackleton et al. 2000; Johnson 2002) because it would account for the staggered arrival and departure of individuals to and from the wintering grounds over the primary sampling occasion. We expect that relaxing this closure assumption will increase our detection probability estimates, as individuals that have not yet arrived at the wintering grounds early in the winter season can be counted as unavailable for capture rather than available but undetected, which should in turn increase precision in survival probability estimates.

TASK 2: STABLE ISOTOPE ANALYSIS OF FEATHER SAMPLES

Background

Analysis of hydrogen stable isotopes in feather samples is a widely-used tool to infer an individual bird's breeding origin (location) to evaluate migratory connectivity patterns. The ratio of deuterium (^2H) to protium (^1H), or the stable hydrogen isotope delta value ($\delta^2\text{H}$, reported in *parts per mille*, or “‰” units), of precipitation varies consistently with latitude and elevation such that $\delta^2\text{H}$ values are lower, or more negative, at higher latitudes and higher elevations (Hobson & Wassenaar 1997; Meehan et al. 2004). The $\delta^2\text{H}$ value of precipitation in a particular location is reflected in tissues (such as feathers) grown there as a result of water and nutrient uptake during tissue formation (Bowen et al. 2005; Wunder 2012). Because Rosy-Finches undergo complete molts each breeding season (Pyle 1997), a feather collected during the winter, when Rosy-Finches can be much more readily located and captured, is assumed to have been grown on the breeding grounds during the preceding breeding season. We can thus infer breeding locations of individuals by generating probability-of-origin maps (Campbell et al. 2020) based on the $\delta^2\text{H}$ value of

feathers sampled during winter and the published $\delta^2\text{H}$ values of water samples from known locations.

In conjunction with our work assessing breeding origins, we have conducted an additional study investigating the variation in $\delta^2\text{H}$ values within individual feathers, or “intra-feather variation”. The goal of this study was to determine whether the section of the feather analyzed impacts the resulting $\delta^2\text{H}$ value for that feather, for which there is evidence in other studies (e.g., Wassenaar and Hobson 2006, Gordo 2020), and which would provide greater context for interpreting of our breeding origin results.

Methods

To prepare feather samples for hydrogen stable isotope analysis, we first allowed collected feathers (right 5th rectrix from Rosy-Finches captured at Sandia Mountains site as described above) along with in-house laboratory standards (supplied by University of New Mexico’s Center for Stable Isotopes [UNM CSI]) to acclimate to the atmospheric conditions of southern New Mexico by storing them in a dry place at room temperature for at least two weeks. We followed Chew et al.’s feather cleaning protocol (Chew et al. 2019) and removed the calamus (Fig. 4a) prior to cleaning to preserve any genetic material contained within. We then swirled feathers in a solution of 2:1 chloroform-methanol for 30 seconds and allowed feathers to dry on a clean paper towel for 24–36 hours. Once dry, we swirled feathers in a solution of 30:1 deionized water and Versa-Clean detergent for 30 seconds followed by three beakers of deionized water for 30 seconds each. Feathers were allowed to dry for another 24–36 hours.

To subsample feathers, we used a scalpel to remove the distal-most ~0.5 cm of the feather including the rachis, weighed out 0.200–0.300 mg of material with a 0.001 mg precision microbalance (Mettler Toledo XPE26), and placed the material in a 3.5×5 mm silver capsule (Costech Analytical Technologies, California). Capsules containing feather material were folded into a small cube and placed in a 96-well ELISA plate and sent to UNM CSI for analysis. For every 23 samples we prepared, we prepared one duplicate sample (i.e., a second capsule of material from a single feather) for quality control. At UNM CSI, samples were run through an elemental analyzer-isotope ratio mass spectrometer (EA-IRMS) along with three in-house laboratory standards (powdered moose fur, powdered goose down, and powdered Florida cow liver) acclimatized to the same conditions as the feather samples and a $\delta^2\text{H}$ value was generated for each sample. In-house laboratory standards were calibrated to international reference materials (USGS standards KHS [Kudu Horn Standard] -35.3‰ and CBS [Caribou Hoof Standard] -157.0‰; (Coplen 2020a,

2020b). All $\delta^2\text{H}$ values are reported relative to the Vienna Standard Mean Ocean Water–Standard Light Antarctic Precipitation (VSMOW–SLAP) scale.

We compared the resulting $\delta^2\text{H}$ values across the three species using a Welch’s ANOVA test (chosen due to a violation in the assumption of equal variances across species) followed by Tukey post-hoc pairwise comparisons. We then compared $\delta^2\text{H}$ values between age classes within each species using a t-test for GCRF and a Wilcoxon rank-sum test (due to the data violating of the assumption of normality) for BCRF and BLRF. To compare $\delta^2\text{H}$ values between sexes within species, we used t-tests for BLRF and GCRF and a Wilcoxon rank-sum test for BCRF, in which the normality assumption was violated.

We then generated probability-of-origin maps for each analyzed feather based on a transfer function developed by Campbell et al. (2025). This transfer function links $\delta^2\text{H}$ values of feathers with average $\delta^2\text{H}$ values of precipitation across North America in August and September (when Rosy-Finch molt occurs) to account for changes that occur in isotope ratios when water molecules are processed through multiple trophic levels. With this function, we can assign a sampled feather to the latitudinal and elevational range in North America it is most likely to have originated from. This transfer function was based on $\delta^2\text{H}$ values of known-origin feathers from ground foraging, short-distance migrants as found by Hobson et al. (2012). We used the R packages *isocat* (Campbell 2020), *terra* (Hijmans 2025a), and *raster* (Hijmans 2025b) to create breeding origin assignment maps.

To test for intra-feather variation in $\delta^2\text{H}$ values, we subsampled feathers from 21 BCRF and 21 GCRF adults at five locations on the feather (Fig. 4b). We compared $\delta^2\text{H}$ values across longitudinal vane-only sections (A1, B1, & C1) within each species using repeated measures ANOVA followed by post-hoc pairwise comparisons. We then used paired T-tests to compare $\delta^2\text{H}$ values between vane only and rachis-containing sections (A1 & A2, B1 & B2) as well as between longitudinal sections containing rachis material (A2 & B2). All analyses were performed in program R version 4.4.3 (R Core Team 2025).

Results

We ran a total of 1288 samples from 828 unique Rosy-Finch feathers collected from individuals wintering at the Sandia Mountains site during 2005–2022 (additional feathers collected during 2023–2025 have been prepared and delivered to UNM CSI and are awaiting analysis). For the 828 feathers sampled, mean $\delta^2\text{H}$ for adult BCRF was -62.8 ± 12.5 (SD) ‰ and for juvenile BCRF was -78.0 ± 13.3 ‰, mean $\delta^2\text{H}$ for adult BLRF was -85.8 ± 15.5 ‰ and for juvenile BLRF was -102.9 ± 14.3 ‰, and mean $\delta^2\text{H}$ for adult GCRF was -119.4 ‰ (± 19.2) and for juvenile GCRF was -130.8 ‰ (± 16.8). $\delta^2\text{H}$ values differed

significantly among the three species ($p < 0.0001$ across all species and in each pairwise comparison of species) and between age classes of each individual species ($p < 0.0001$ for all three species; Fig. 5). Species differences were consistent with differences in breeding ranges; GCRF, which breed in the northernmost latitudes, had the lowest (most negative) $\delta^2\text{H}$ values while BCRF, which breed in the southernmost areas had the highest (least negative) $\delta^2\text{H}$ values. The differences we observed in $\delta^2\text{H}$ between ages (juveniles consistently more negative than adults on average) could be attributed to differences in timing of feather growth or differences in diet during feather growth (Langin et al. 2007). Adults may derive hydrogen directly from local drinking water which has a higher $\delta^2\text{H}$ value compared to plant and animal tissues in the same location. It cannot be ruled out that differences in $\delta^2\text{H}$ between age classes could reflect differences in breeding origins between adults and juveniles of these species.

We did not find significant differences in $\delta^2\text{H}$ values between sexes in any of the three species ($p = 0.757$ for BCRF, $p = 0.171$ for BLRF, and $p = 0.619$ for GCRF; Fig. 6). Over 17 years of feather collection, $\delta^2\text{H}$ values trended positively over time in BLRF ($\beta = 0.719$, 95% confidence interval [CI]: 0.242–1.196) and GCRF ($\beta = 1.508$, 95% CI: 1.059–1.957) but not in BCRF ($\beta = -0.206$, 95% CI: -0.650–0.238; Fig. 7). This indicates either a trend toward more southerly and/or lower elevation breeding origins of wintering individuals with time in the two longer-ranging Rosy-Finch species (i.e., BLRF and GCRF); however, trends may instead be related to fluctuations in weather conditions on breeding grounds.

Maps for BCRF adult and juvenile individuals suggest breeding origins in the northern, central, and southern regions of the species' range (Fig. 8). Of the individual Rosy-Finches from which feathers were sampled and analyzed, 53 individuals were captured and sampled during multiple distinct winter seasons, and 26 of these individuals were sampled during multiple distinct winter seasons as adults (Fig. 9). We plan to use these data from recaptured individuals to assess the extent to which individuals wintering at the Sandia Mountains site exhibit site fidelity between breeding seasons. Furthermore, using the maps we generated, ongoing work is summarizing the likely breeding origins of Rosy-Finches wintering in New Mexico by grouping maps with similar patterns, which should allow us to identify particular breeding areas that are connected to the Sandia Mountains as habitat used by Rosy-Finches. We also are further refining our feather–precipitation $\delta^2\text{H}$ transfer function by incorporating analyses of BCRF feathers collected during the breeding season as part of other Rosy-Finch studies. Incorporating $\delta^2\text{H}$ values from these feathers should allow us to more accurately link our $\delta^2\text{H}$ values from feathers of unknown origin to $\delta^2\text{H}$ values of precipitation compared to our current transfer function which includes data from birds in the same foraging and migratory guild as Rosy-Finches, but not from Rosy-Finches themselves. By broadly identifying the areas where Rosy-

Finches wintering in New Mexico breed and patterns in their breeding origins over time, we expect that the results of this study may help New Mexico Department of Game and Fish to make connections with agencies that manage habitat Rosy-Finches use during other parts of the year to coordinate conservation efforts across the species' entire annual cycle. Knowing where individuals are breeding could provide context for any changes in demographic rates of these species on their wintering grounds.

Mean $\delta^2\text{H}$ values for BCRF feather subsections were -60.9 ± 14.3 (SD) ‰ for A1, -62.1 ± 15.1 ‰ for A2, -61.8 ± 14.3 ‰ for B1, -65.8 ± 14.2 ‰ for B2, and -61.3 ± 9.6 ‰ for C1. Mean $\delta^2\text{H}$ values for GCRF were -111.6 ± 17.9 ‰ for A1, -113.0 ± 18.1 ‰ for A2, -115.0 ± 18.6 ‰ for B1, -118.9 ± 19.1 ‰ for B2, and -115.3 ± 21.1 ‰ for C1. We found that sections excluding feather rachis subsampled longitudinally (A1, B1, and C1; Fig. 4b) in BCRF did not result in significantly different $\delta^2\text{H}$ values ($p = 0.722$) but did vary significantly in GCRF between A1 and B1 ($p < 0.0001$) and between A1 and C1 ($p = 0.001$; Fig. 10a). The $\delta^2\text{H}$ values of longitudinal sections containing rachis material (A2 and B2) were significantly different in both BCRF and GCRF ($p < 0.0001$ in both species; Fig. 10b). In all cases, $\delta^2\text{H}$ values became increasingly negative as samples were taken from the distal to the proximal end of the feather (Fig. 4a). Lateral comparisons of sections with and without rachis material resulted in significantly different $\delta^2\text{H}$ values in both species ($p = 0.00240$ for BCRF A1 vs. A2, $p = 0.0371$ for GCRF A1 vs. A2, $p < 0.0001$ for BCRF B1 vs. B2, $p < 0.0001$ for GCRF B1 vs. B2; Fig. 10c-d). In all cases, the $\delta^2\text{H}$ values of sections containing rachis material were more negative than sections with vane material only (by 1.2–4.0 ‰). For our breeding origin analysis, subsamples are taken from the distal-most tip of feathers and include rachis material (Fig. 4a). This work suggests that the longitudinal location of sampling along the feather and the inclusion or exclusion of the rachis may influence a sample's $\delta^2\text{H}$ value, and any products derived from that $\delta^2\text{H}$ value (e.g., breeding origin maps). It does not necessarily matter where on the feather subsamples are taken from as long as $\delta^2\text{H}$ value comparisons are limited to similar sections or appropriate adjustments are made for comparison. This includes correlating feathers of unknown origin to precipitation isotope values—use of a transfer function derived from feathers sampled in a different location could result in less accurate origin assignment. These results allowed us to adjust our breeding origin maps according to where we sampled on the feather as compared to the feather locations sampled in Hobson et al. (2012). We are in the process of carrying out this analysis on a set of 22 BCRF and 23 GCRF juvenile feathers to determine if within-feather variation patterns vary by age.

We are also in the process of analyzing multiple feathers collected from the tails of single Rosy-Finch individuals during the 2023–2024 and 2024–2025 winter seasons at the Sandia Mountains site. Examining inter-feather (between feather) variation in $\delta^2\text{H}$ values

within individuals will enable us to determine whether the particular feather sampled from an individual bird (e.g., the 1st or 5th rectrix of the tail) affects the resulting isotope value. Both the intra- and inter-feather variation studies will enable us to better compare our results with those of other studies that may have sampled different feathers or feather sections.

TASK 3: ESTABLISH NEW RFID FEEDERS FOR WINTER MONITORING

Background

Radio frequency identification (RFID)-equipped artificial feeders are increasingly being implemented as a means of monitoring populations because of the feeders' potentially higher bird detection rates and ability to collect more robust data with reduced human effort. Individual birds in a population need to be captured only once to be equipped with an RFID tag; thereafter, tagged birds are detected when they land on or within antenna coils designed to match the tag frequencies. Furthermore, biologists only need to visit the study area occasionally for RFID reader maintenance and data downloading instead of having to regularly sample the bird population. In contrast to active banding mark-recapture monitoring efforts, RFID-tagged birds can be detected by RFID readers at any time of day and on any day during deployment of the reader with no impact of human activity on natural bird behavior. We aimed to assess whether this technology could be used to monitor Rosy-Finches on their wintering grounds in NM to supplement active mark-recapture efforts during the winter season, providing improved detection rates and thus more precise survival estimates.



Radio frequency identification (RFID) reader antenna coils within feeder tray (left) and fully assembled feeder with additional solid plastic layer added atop coils for protection from elements and rodents and covered with seed (right). Photos by Corrie Borgman, USFWS.

Methods

An RFID reader apparatus consists of Electronic Transponder Analysis Gateway (ETAG) readers powered by 6,400 mAh USB battery packs and 3.5 Watt 6 V solar panel arrays (voltaicsystems.com). These readers detect low-frequency (125 kHz) RFID tags affixed to the legs of tagged Rosy-Finches. Largely based on trial and error, we utilized numerous iterations of feeder and antenna designs to reach an optimal design because antennae were frequently damaged from squirrels chewing on the apparatus and memory card performance was not at desired levels. The final feeder design for 2023–2024 involved “sandwiching” antenna coils between two sheets of plastic, which minimized the ability of squirrels to access sensitive antennae but still allowed for tag detection. This was a successful strategy, and feeders incurred minimal squirrel damage over the season. In addition, memory card performance was improved by updating the card housing to include a more robust weatherproof design with less need to move componentry.

We deployed an RFID-equipped feeder at the Sandia Mountains site, NM (SACR) during three winter/spring periods: 20 January–10 April 2023, 29 November 2023–19 April 2024, and 1 December 2024–10 April 2025. A similar feeder was deployed at a private condominium in Taos Ski Valley (TSV), NM during two periods: 9 January–3 May 2024 and 15 January–19 May 2025.

To compare RFID-collected data to active banding data, we conducted two robust design survival analyses (see methods above) over 2022–2025, using all collected RFID data and a subset of the active mark-recapture data that overlapped the same period. We included age class as a covariate on the survival parameter, but combined data from all species due to sparse data from certain species. We only included individuals in the RFID analysis that were detected by RFID at least once. We divided active mark-recapture data into two-week secondary sampling occasions (as above) but used individual day as the secondary sampling occasion for the RFID data analysis for a total of 110 secondary sampling occasions within each winter season.

Results

We marked a total of 353 individual Rosy-Finches (42 BCRF, 275 BLRF, and 36 GCRF) with RFID tags at SACR and TSV during this study. Of these, 199 individuals were detected via the RFID reader. At SACR, 141 new individuals (0 BCRF, 110 BLRF, 31 GCRF) were captured and tagged during the 2024–2025 winter season. No tagging effort occurred at TSV in 2024–

2025 due to a lack of Rosy-Finches reported in the area during this time. Six BLRF that were originally tagged at SACR during the 2022–2023 winter season were detected by RFID in 2023–2024, eight BLRF tagged at SACR in 2023–2024 were detected by RFID in 2024–2025, and two BLRF originally tagged at SACR in 2022–2023 were detected by RFID in 2024–2025. A single BLRF individual originally RFID-tagged in 2022–2023 was detected again in both 2023–2024 and 2024–2025. Detections occurred at the highest rates at SACR at 07:00, 11:00, and 15:00 and at TSV at 10:00, and in the months of January, February, and March at both sites and across years (Fig.11).

In our robust design survival analysis of RFID data, we found mean juvenile survival to be 0.67 (95% CrI: 0.17–1.00) and mean adult survival to be 0.47 (95% CrI: 0.10–1.00). Detection probabilities ranged from 0.003 to 0.47. In our comparative analysis of mark-recapture data 2022–2025, mean juvenile survival was 0.62 (95% CrI: 0.06–1.00), mean adult survival was 0.03 (95% CrI: 0.00–0.34), and detection probabilities ranged from 0.02 to 0.49. Although these numbers are very different from what we would expect for juvenile and adult migratory passerines (see Task 1 above), high variation around the mean estimates suggests lack of precision, likely due to sparse data. Detection probabilities were comparable between the two analyses but mean adult survival in the RFID-based analysis was much closer to what we would expect (and what we estimated with many more years of data in Task 1) than were the results of the active mark-recapture-based analysis.

The RFID data collection approach has the potential to provide a large amount of data that is not possible to collect with banding alone. Although our ability to thoroughly assess the efficacy of this technology is limited, it appears that RFID data may improve demographic estimates in a population for a study of limited duration. Another advantage is that RFID data can be used beyond demographic analysis to address questions of temporal activity in a population, which can provide information on migratory timing and patterns. If scaled up to span a greater number of wintering and stopover sites, this approach could be combined with traditional mark-recapture efforts to greatly increase our understanding of migratory patterns in these elusive species.

CONCLUSION

While further investigation is still needed in certain areas of this research to reach more firm conclusions, this study provides valuable insight into a variety of aspects of Rosy-Finch ecology. First, based on our robust design survival analysis (Task 1), annual survival

probabilities of Rosy-Finches wintering in New Mexico were lower in GCRF than in BCRF and BLRD, and were overall low compared to those of other high-elevation obligate and migratory passerines. Trends were inconsistent between age groups of each of the three species included in this study, but inclusion of additional covariates and more complex modeling structures may improve our confidence in our estimates. Our hydrogen stable isotope analysis (Task 2) revealed that Brown-capped Rosy-Finches wintering in New Mexico likely originate from a variety of locations across their breeding range, that $\delta^2\text{H}$ values of juveniles wintering in New Mexico are consistently more negative than those of adults, and that $\delta^2\text{H}$ values in two of the species—BLRF and GCRF—show an increasing trend over time. Our work comparing $\delta^2\text{H}$ values from different subsections of Rosy-Finch feathers indicates that it is important to consider where on feathers samples are taken from and to pay attention to sampling section when comparing values across studies. Furthermore, our RFID analysis (Task 3) shows that RFID monitoring can be useful in improving detection probability and consequently the precision of survival estimates in species such as Rosy-Finches, particularly in the short-term.

ACKNOWLEDGEMENTS

Funding for this project was provided by the Share with Wildlife program of the New Mexico Department of Game and Fish, State Wildlife Grant #T-79-R-1. We thank the many individuals who assisted with the Sandia Mountains field work, including Nancy Cox, Asher Gorbet, Jason Kitting, Amber West, and Laura West. We further thank Alexes Albillar, Cynthia Dunkleberger, Kadence Presser, Gwen Smith, and Emma Varela for their assistance in the lab preparing feather samples. Erin Duvuvuei was instrumental in the RFID component of this work. We thank Karen H. Gaines for editing assistance with this and previous project reports. Any use of trade, firm, or product names is for descriptive purposes only and does not imply endorsement by the U.S. Government.

REFERENCES

- Alerstam T, Bäckman J. 2018. Ecology of animal migration. *Current Biology* **28**:R968–R972.
- Bowen GJ, Wassenaar LI, Hobson KA. 2005. Global application of stable hydrogen and oxygen isotopes to wildlife forensics. *Oecologia* **143**:337–348.
- Brooks SP, Gelman A. 1998. General Methods for Monitoring Convergence of Iterative Simulations. *Journal of Computational and Graphical Statistics* **7**:434–455.
- Campbell C, Gardner J, Rushing C, Farr C, Norvell R, Savides K. 2025. Quantifying rosy-finch migration with stable hydrogen isotope feather markers highlights the need for

- inter-state collaboration to reach conservation goals. *Avian Conservation and Ecology* **20**:art6.
- Campbell CJ. 2020. isocat: Isotope Origin Clustering and Assignment Tools. Available from <https://CRAN.R-project.org/package=isocat>.
- Campbell CJ, Fitzpatrick MC, Vander Zanden HB, Nelson DM. 2020. Advancing interpretation of stable isotope assignment maps: comparing and summarizing origins of known-provenance migratory bats. *Animal Migration* **7**:27–41.
- Chew B, Kelly J, Contina A. 2019. Stable isotopes in avian research: a step by step protocol to feather sample preparation for stable isotope analysis of carbon ($\delta^{13}\text{C}$), nitrogen ($\delta^{15}\text{N}$), and hydrogen ($\delta^2\text{H}$). Version 1.1 v1. preprint. Available from <https://www.protocols.io/view/stable-isotopes-in-avian-research-a-step-by-step-p-z2uf8ew> (accessed March 13, 2023).
- Coplen TB. 2020a. Report of Stable Isotopic Composition: Reference Material KHS (Kudu Horn Standard). USGS Reston Stable Isotope Laboratory.
- Coplen TB. 2020b. Report of Stable Isotopic Composition: Reference Material CBS (Caribou Hoof Standard). USGS Reston Stable Isotope Laboratory.
- Fink D et al. 2022. eBird Status and Trends, Data Version: 2021; Released: 2022. Cornell Lab of Ornithology, Ithaca, New York.
- Gordo O. 2020. Stable hydrogen isotope measurements of songbird feathers: effects of intra-feather variability and sample processing. *Journal of Ornithology* **161**:381–388.
- Grace J, Berninger F, Nagy L. 2002. Impacts of Climate Change on the Tree Line. *Annals of Botany* **90**:537–544.
- Grüebler MU, Korner-Nievergelt F, Naef-Daenzer B. 2014. Equal nonbreeding period survival in adults and juveniles of a long-distant migrant bird. *Ecology and Evolution* **4**:756–765.
- Hijmans RJ. 2025a. terra: Spatial Data Analysis. Available from <https://CRAN.R-project.org/package=terra>.
- Hijmans RJ. 2025b. raster: Geographic Data Analysis and Modeling. Available from <https://CRAN.R-project.org/package=raster>.
- Hobson KA, Van Wilgenburg SL, Wassenaar LI, Larson K. 2012. Linking Hydrogen ($\delta^2\text{H}$) Isotopes in Feathers and Precipitation: Sources of Variance and Consequences for Assignment to Isoscapes. *PLoS ONE* **7**:e35137.
- Hobson KA, Wassenaar LI. 1997. Linking breeding and wintering grounds of neotropical migrant songbirds using stable hydrogen isotopic analysis of feathers. *Oecologia* **109**:142–148.
- Holmes RT. 2007. Understanding population change in migratory songbirds: long-term and experimental studies of Neotropical migrants in breeding and wintering areas. *Ibis* **149**:2–13.
- Johnson R, Hendricks P, Pattie D, Hunter K. 2000. Brown-capped Rosy-Finch. Pages 1–25 *The Birds of North America*. Cornell Laboratory of Ornithology and the Academy of Natural Sciences.
- Johnson RE. 2002. Black Rosy-Finch. Pages 1–27 *The Birds of North America*. Cornell Laboratory of Ornithology and the Academy of Natural Sciences.
- Julyan R, Stuever M. 2005. *Field Guide to the Sandia Mountains*. UNM Press.

- Kellner K. 2024. jagsUI: A Wrapper Around “rjags” to Streamline “JAGS” Analyses. Available from <https://CRAN.R-project.org/package=jagsUI>.
- Kendall WL, Bjorkland R. 2001. Using Open Robust Design Models to Estimate Temporary Emigration from Capture-Recapture Data. *Biometrics* **57**:1113–1122.
- Kendall WL, Nichols JD, Hines JE. 1997. Estimating Temporary Emigration Using Capture-Recapture Data with Pollock’s Robust Design. *Ecology* **78**:563–578.
- Kendall WL, Pollock KH, Brownie C. 1995. A Likelihood-Based Approach to Capture-Recapture Estimation of Demographic Parameters under the Robust Design. *Biometrics* **51**:293–308. International Biometric Society.
- Klaassen RHG, Hake M, Strandberg R, Koks BJ, Trierweiler C, Exo K-M, Bairlein F, Alerstam T. 2014. When and where does mortality occur in migratory birds? Direct evidence from long-term satellite tracking of raptors. *Journal of Animal Ecology* **83**:176–184.
- Langin KM, Reudink MW, Marra PP, Norris DR, Kyser TK, Ratcliffe LM. 2007. Hydrogen Isotopic Variation in Migratory Bird Tissues of Known Origin: Implications for Geographic Assignment. *Oecologia* **152**:449–457. Springer.
- Latimer CE, Gardner JH. 2022. Leveraging RFID-enabled bird feeders to monitor Rosy-Finch phenology and demographics. Bird Conservancy of the Rockies and Sageland Collaborative.
- Lebreton J-D, Burnham KP, Clobert J, Anderson DR. 1992. Modeling Survival and Testing Biological Hypotheses Using Marked Animals: A Unified Approach with Case Studies. *Ecological Monographs* **62**:67–118.
- MacDougall-Shackleton SA, Johnson RE, Hahn TP. 2000. Gray-crowned Rosy-Finch. Pages 1–15 *Birds of North America*. Cornell Laboratory of Ornithology and the Academy of Natural Sciences.
- McKim-Louder MI, Hoover JP, Benson TJ, Schelsky WM. 2013. Juvenile Survival in a Neotropical Migratory Songbird Is Lower than Expected. *PLoS ONE* **8**:e56059.
- Meehan TD, Giermakowski JT, Cryan PM. 2004. GIS-based model of stable hydrogen isotope ratios in North American growing-season precipitation for use in animal movement studies. *Isotopes in Environmental and Health Studies* **40**:291–300.
- Pakanen V-M et al. 2018. Cold weather increases winter site fidelity in a group-living passerine. *Journal of Ornithology* **159**:211–219.
- Paxton EH, Durst SL, Sogge MK, Koronkiewicz TJ, Paxton KL. 2017. Survivorship across the annual cycle of a migratory passerine, the willow flycatcher. *Journal of Avian Biology* **48**:1126–1131.
- Pepin N, Diaz HF, Bradley RS, Baraer M. 2015. Elevation-dependent warming in mountain regions of the world. *Nature Climate Change* **5**:424–430.
- Plummer M. 2024. rjags: Bayesian Graphical Models using MCMC. Available from <https://CRAN.R-project.org/package=rjags>.
- Pollock KH. 1982. A Capture-Recapture Design Robust to Unequal Probability of Capture. *The Journal of Wildlife Management* **46**:752–757. [Wiley, Wildlife Society].
- Pyle P. 1997. Identification Guide to North American Birds, Part I. Slate Creek Press, Bolinas, CA, USA.

- R Core Team. 2025. R: A Language and Environment for Statistical Computing. R Foundation for Statistical Computing, Vienna, Austria. Available from <https://www.R-project.org/>.
- Redmond LJ, Murphy MT. 2012. Using complementary approaches to estimate survival of juvenile and adult Eastern Kingbirds. *Journal of Field Ornithology* **83**:247–259. [Association of Field Ornithologists, Wiley].
- Riecke TV, Leach AG, Gibson D, Sedinger JS. 2018. Parameterizing the robust design in the BUGS language: Lifetime carry-over effects of environmental conditions during growth on a long-lived bird. *Methods in Ecology and Evolution* **9**:2294–2305.
- Rockwell SM, Wunderle JM, Sillett TS, Bocetti CI, Ewert DN, Currie D, White JD, Marra PP. 2017. Seasonal survival estimation for a long-distance migratory bird and the influence of winter precipitation. *Oecologia* **183**:715–726.
- Rosenberg KV et al. 2019. Decline of the North American avifauna. *Science* **366**:120–124.
- Schaub M, Royle JA. 2014. Estimating true instead of apparent survival using spatial Cormack–Jolly–Seber models. *Methods in Ecology and Evolution* **5**:1316–1326.
- Somershoe SG, Brown CRD, Poole RT. 2009. Winter Site Fidelity and Over-Winter Site Persistence of Passerines in Florida. *The Wilson Journal of Ornithology* **121**:119–125. Wilson Ornithological Society.
- Strinella E, Scridel D, Brambilla M, Schano C, Korner-Nievergelt F. 2020. Potential sex-dependent effects of weather on apparent survival of a high-elevation specialist. *Scientific Reports* **10**:8386.
- USFWS. 2021. Birds of Conservation Concern 2021. U.S. Department of Interior, Falls Church, Virginia. Available from <https://www.fws.gov/media/birds-conservation-concern-2021pdf>.
- Wassenaar LI, Hobson KA. 2006. Stable-hydrogen isotope heterogeneity in keratinous materials: mass spectrometry and migratory wildlife tissue subsampling strategies. *Rapid Communications in Mass Spectrometry* **20**:2505–2510.
- Western Regional Climate Center. 2025. Cooperative Climatological Data Summaries. Available from <https://wrcc.dri.edu/cgi-bin/cliMAIN.pl?nm8011> (accessed May 14, 2025).
- Wunder MB. 2012. Determining geographic patterns of migration and dispersal using stable isotopes in keratins. *Journal of Mammalogy* **93**:360–367.

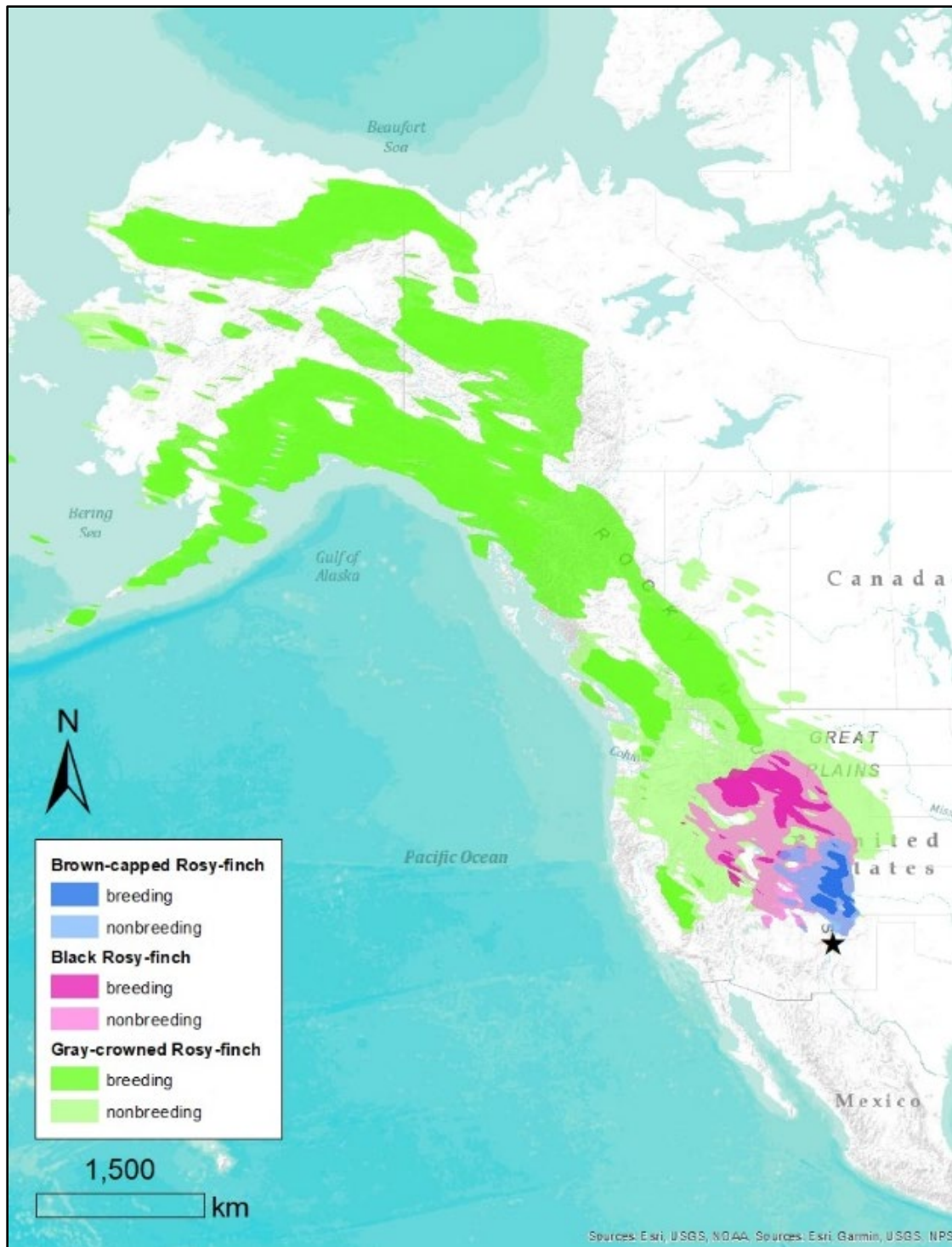


Figure 1. Distributions of the three North American Rosy-Finch species. Darker colors represent breeding ranges, and the black star indicates the study site at the Sandia Mountains site in northern New Mexico. Distribution data layers from Fink et al. 2022.

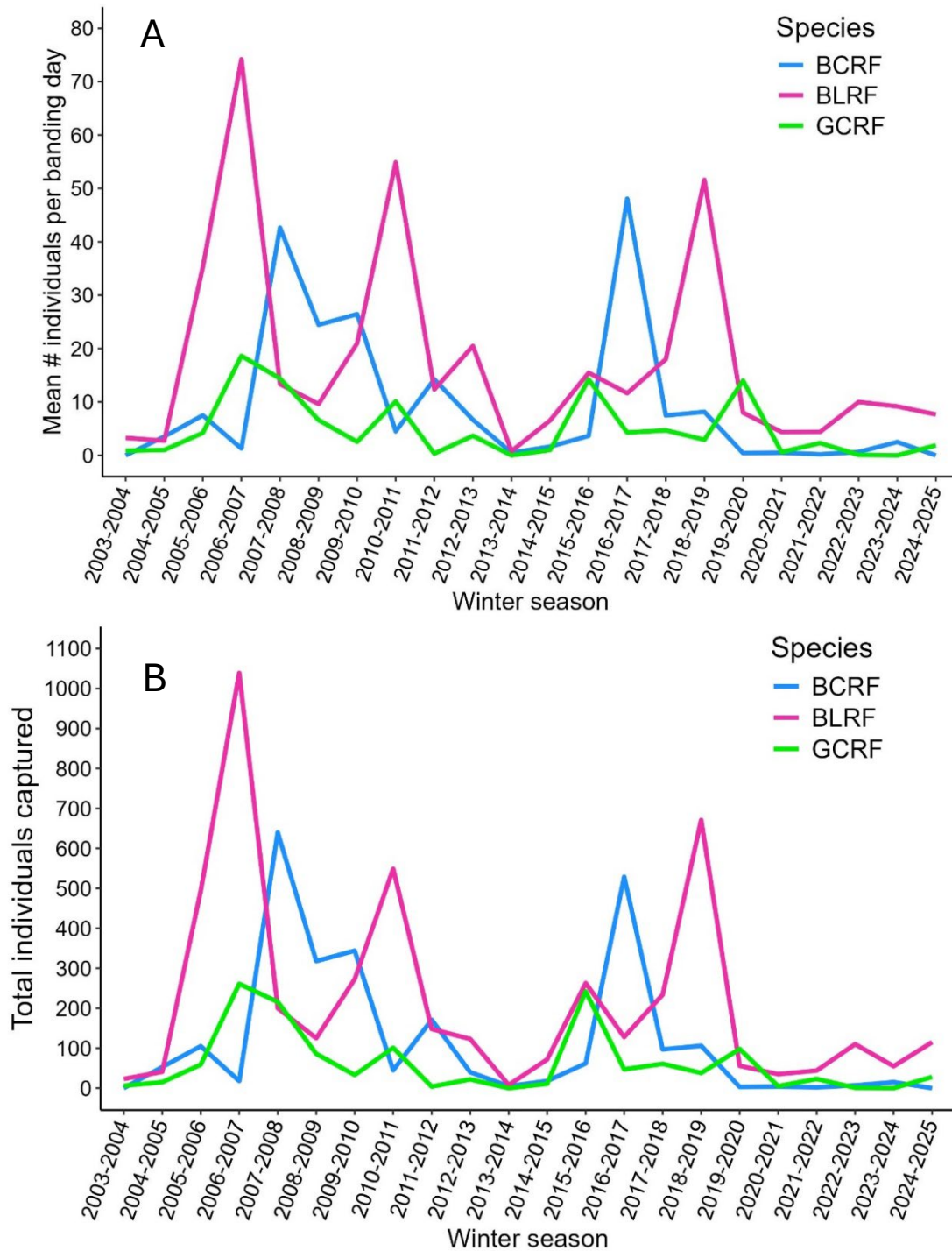


Figure 2. Mean number of unique Rosy-Finches captured in total across winter seasons (A) and averaged across number of banding days per winter season at the Sandia Mountains site, NM, from 2004–2025 (B). Figures include individuals recaptured on multiple banding days within a season and/or across multiple winter seasons. Species abbreviations: Brown-capped Rosy-Finch (*Leucosticte australis*): BCRF; Black Rosy-Finch (*L. atrata*): BLRF; Gray-crowned Rosy-Finch (*L. tephrocotis*): GCRF.

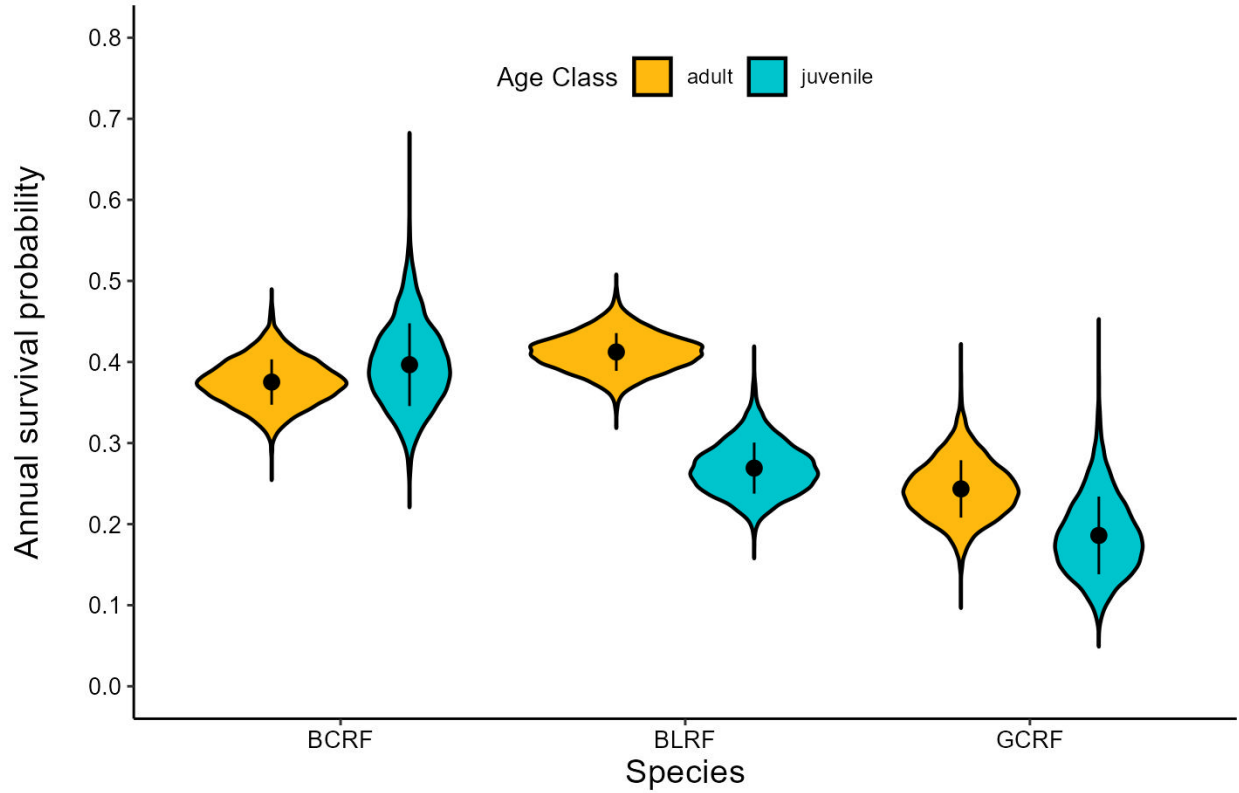


Figure 3. Annual survival estimates for Rosy-Finches overwintering at the Sandia Mountains site, NM from 2004 to 2025 by species and age class. Black dots represent posterior distribution means and error bars reflect the standard deviation. The width of each plot reflects the density of the posterior distribution at each probability value and the extent from top to bottom shows the full range of the posterior distribution. Species abbreviations: Brown-capped Rosy-Finch (*Leucosticte australis*): BCRF; Black Rosy-Finch (*L. atrata*): BLRF; Gray-crowned Rosy-Finch (*L. tephrocotis*): GCRF.

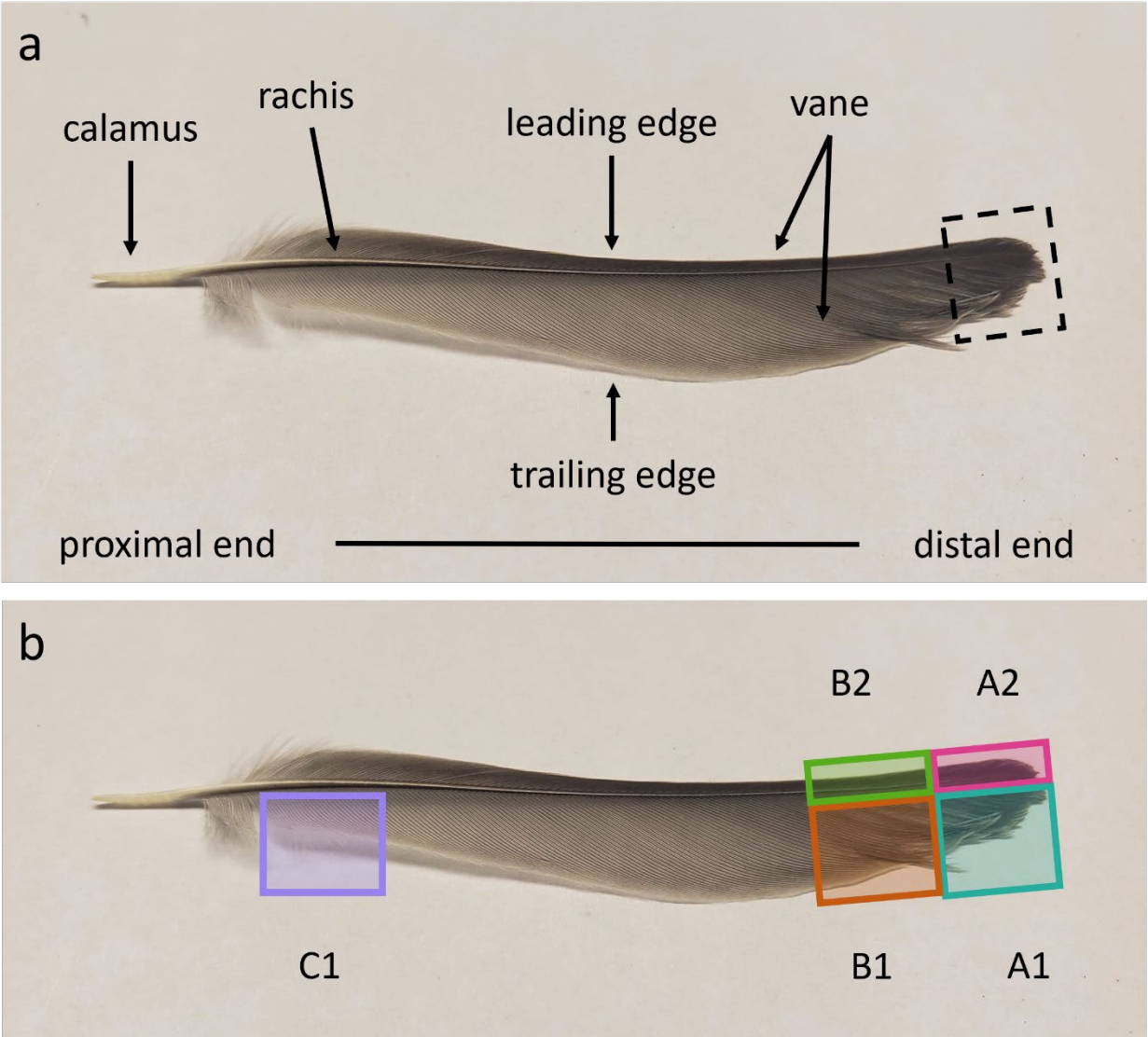


Figure 4. Feather diagrams for stable hydrogen isotope intra-feather variation study. Panel (a) shows general feather anatomy and sampling region for breeding origin analysis (dashed black box); panel (b) shows subsampling delineations for intra-feather variation study. Sections A1, B1, and C1 contain only vane material; sections A2 and B2 contain a combination of vane and rachis material.

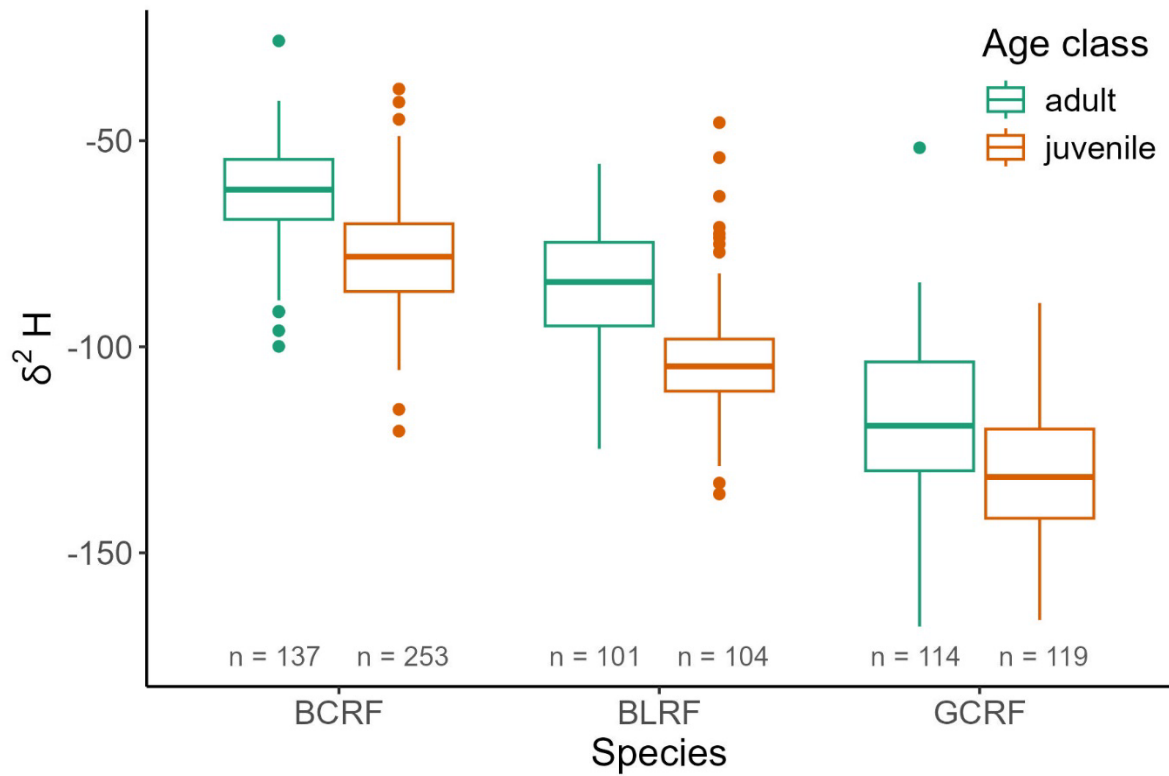


Figure 5. Stable hydrogen isotope ratios ($\delta^2\text{H}$) Rosy-Finch feathers sampled on the Sandia Mountains site, NM from 2004–2022 grouped by species and age group. Species abbreviations: Brown-capped Rosy-Finch (*Leucosticte australis*): BCRF; Black Rosy-Finch (*L. atrata*): BLRF; Gray-crowned Rosy-Finch (*L. tephrocotis*): GCRF.

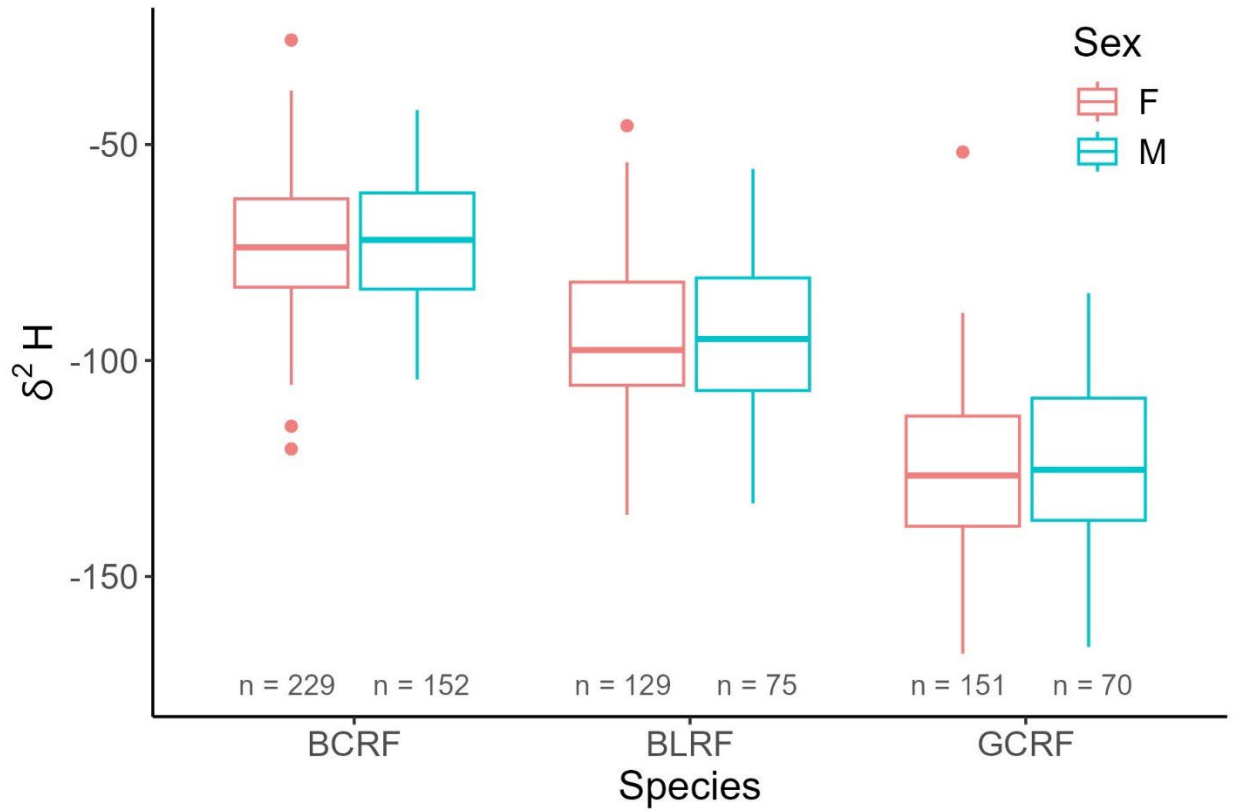


Figure 6. Stable hydrogen isotope ratios ($\delta^2\text{H}$) of Rosy-Finch feathers sampled on the Sandia Mountains site, NM from 2005–2022 grouped by species and sex. Species abbreviations: Brown-capped Rosy-Finch (*Leucosticte australis*): BCRF; Black Rosy-Finch (*L. atrata*): BLRF; Gray-crowned Rosy-Finch (*L. tephrocotis*): GCRF.

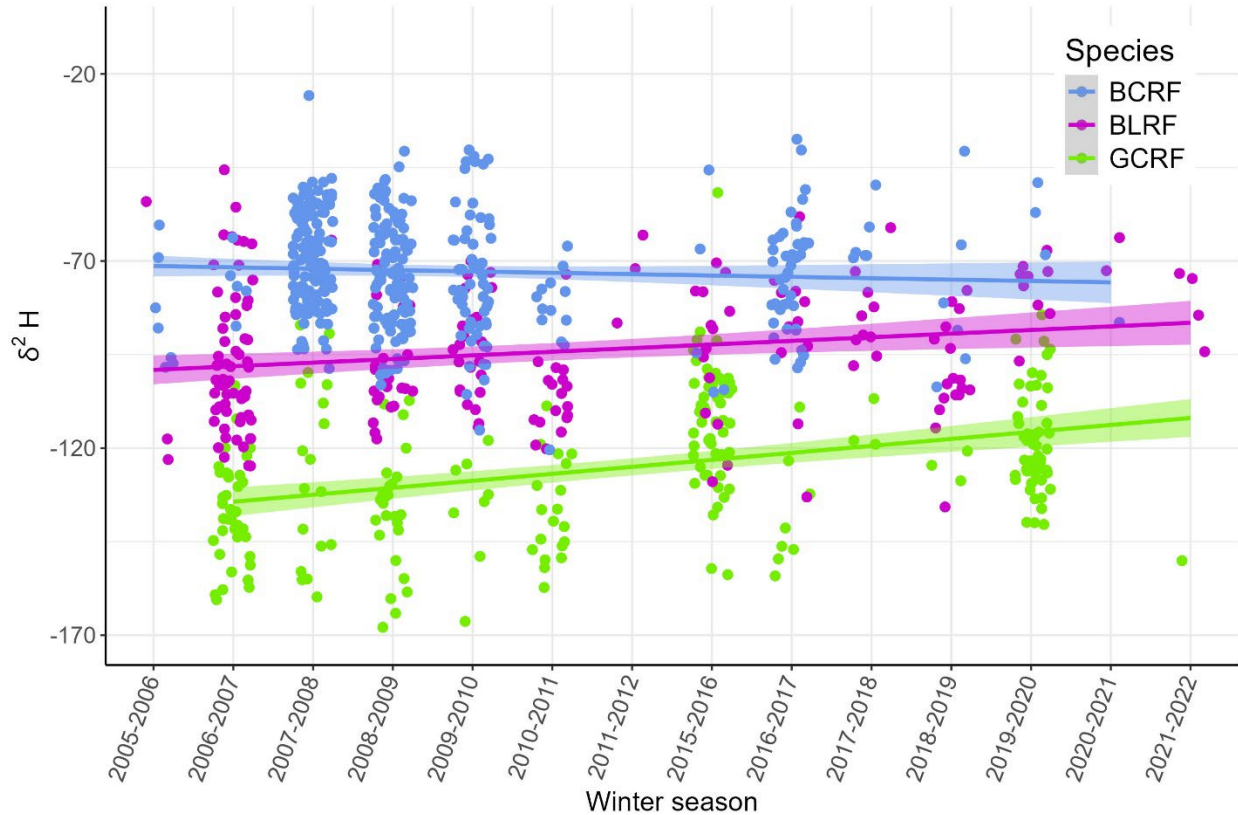


Figure 7. Stable hydrogen isotope ratios ($\delta^2\text{H}$) of individual Rosy-Finch feathers sampled on the Sandia Mountains site, NM from 2005–2022 grouped by winter season of sampling. Each point represents one feather. Trend lines show linear trend of $\delta^2\text{H}$ value with time, in which more negative values indicate higher latitudes and elevations. Species abbreviations: Brown-capped Rosy-Finch (*Leucosticte australis*): BCRF; Black Rosy-Finch (*L. atrata*): BLRF; Gray-crowned Rosy-Finch (*L. tephrocotis*): GCRF.

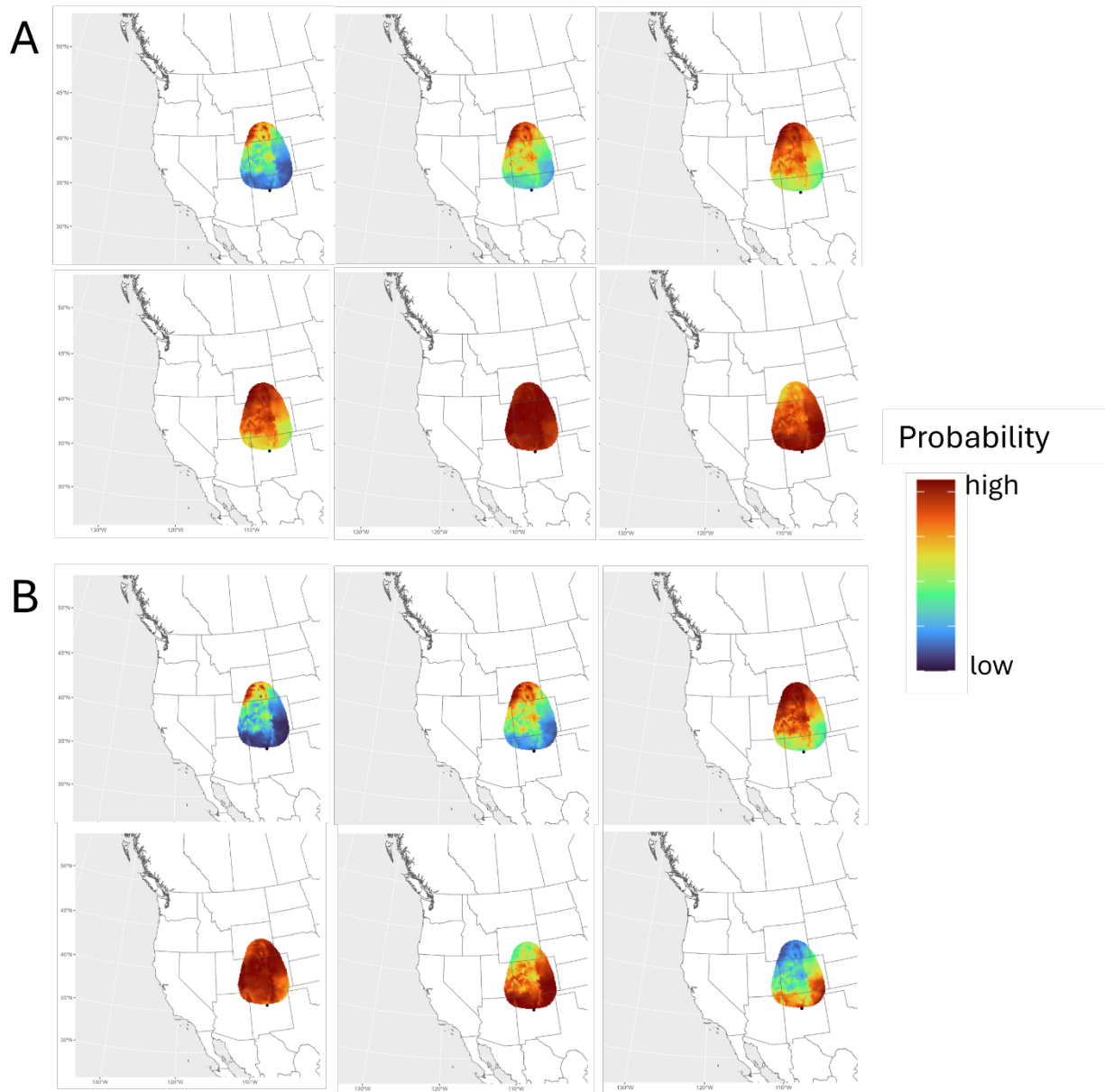


Figure 8. Probability of origin maps for Brown-capped Rosy-Finch (*Leucosticte australis*) juvenile (A) and adult (B) individuals based on stable hydrogen isotope ratio ($\delta^2\text{H}$) of feathers sampled on the Sandia Mountains site, NM from 2005–2022 (black dot). Map values for juveniles have been adjusted by +10‰ to reflect the mean difference of juvenile $\delta^2\text{H}$ values from adult values. Each map represents an individual feather sample and selected maps reflect the range of probability of origin assignments generated for each age class.

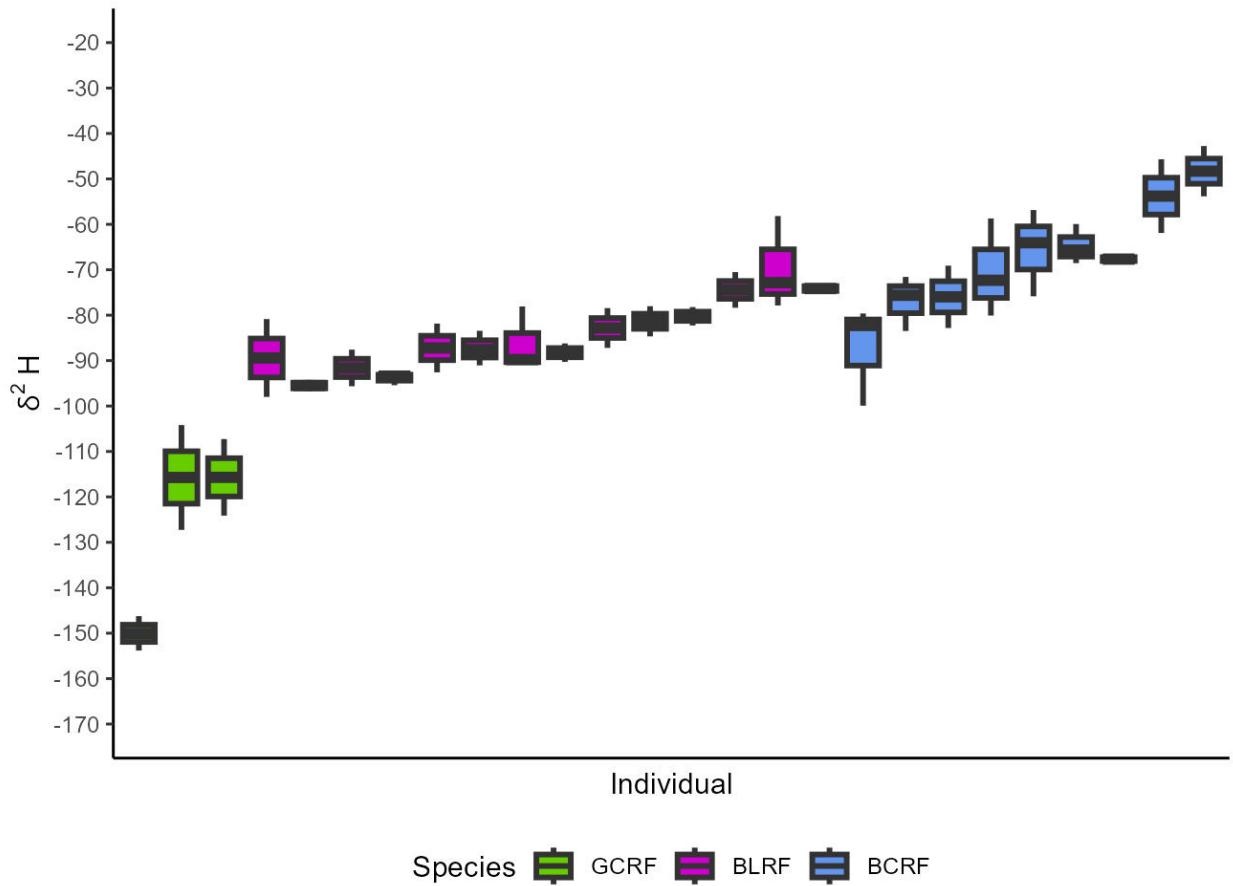


Figure 9. Stable hydrogen isotope ratios ($\delta^2\text{H}$) of Rosy-Finch feathers sampled on the Sandia Mountains site, NM from 2005–2022, grouped by individual. Each individual (26 total) shown was sampled 2–3 times as an adult during distinct winter seasons; individuals are intentionally arranged along the x-axis in order of increasing mean $\delta^2\text{H}$ value. Species abbreviations: Brown-capped Rosy-Finch (*Leucosticte australis*): BCRF; Black Rosy-Finch (*L. atrata*): BLRF; Gray-crowned Rosy-Finch (*L. tephrocotis*): GCRF.

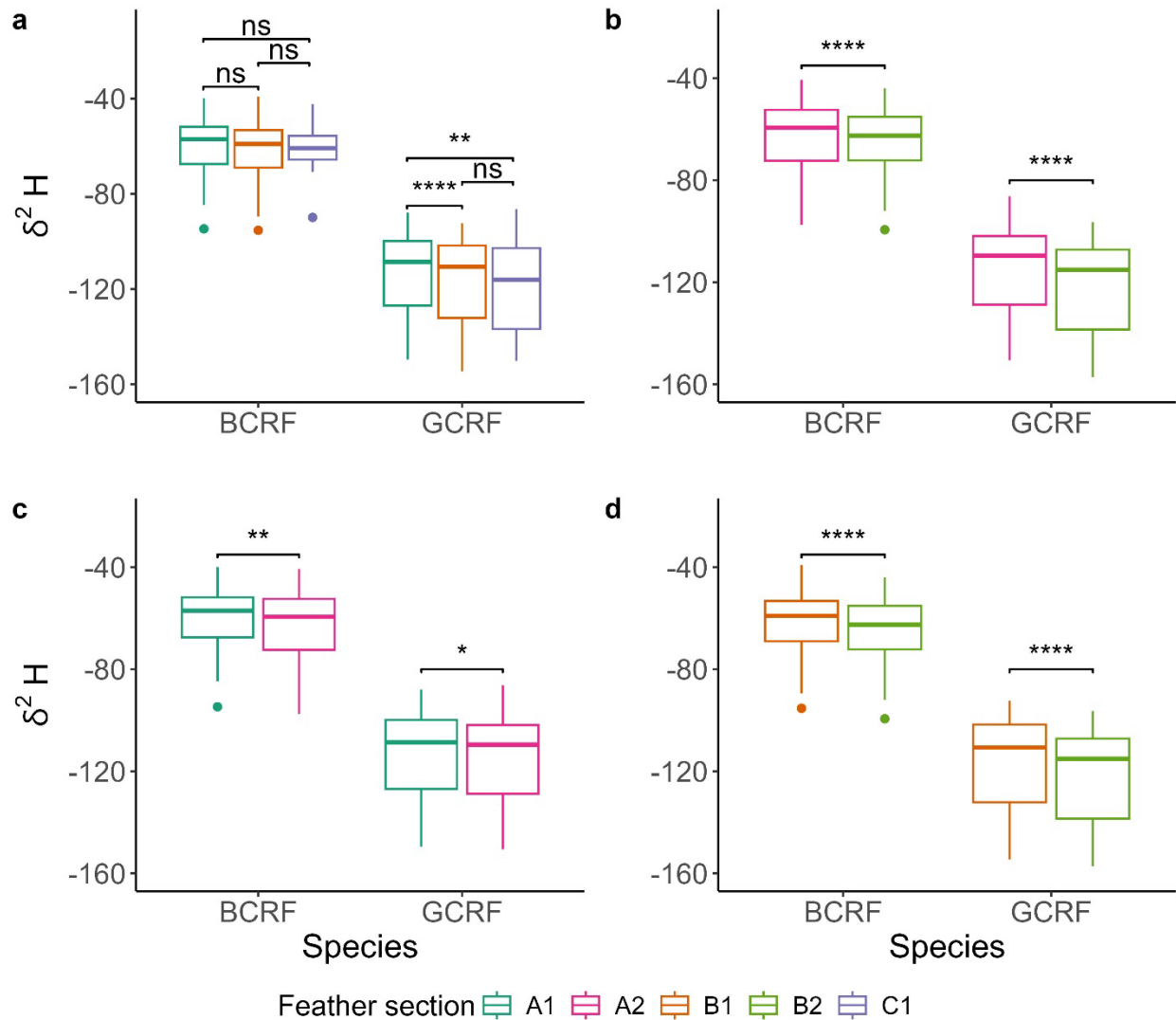


Figure 10. Boxplot and line plots for comparison of stable hydrogen isotope ($\delta^2\text{H}$) values for different sections of Rosy-Finch feathers collected on the Sandia Mountains site, NM from 2007–2020. Feather sections are shown in Figure 4. Panels (a) and (b) compare $\delta^2\text{H}$ values of longitudinal sections; panels (c) and (d) compare values of sections containing rachis material to those containing only vane material. Species abbreviations: Brown-capped Rosy-Finch (*Leucosticte australis*): BCRF; Black Rosy-Finch (*L. atrata*): BLRF; Gray-crowned Rosy-Finch (*L. tephrocotis*): GCRF.

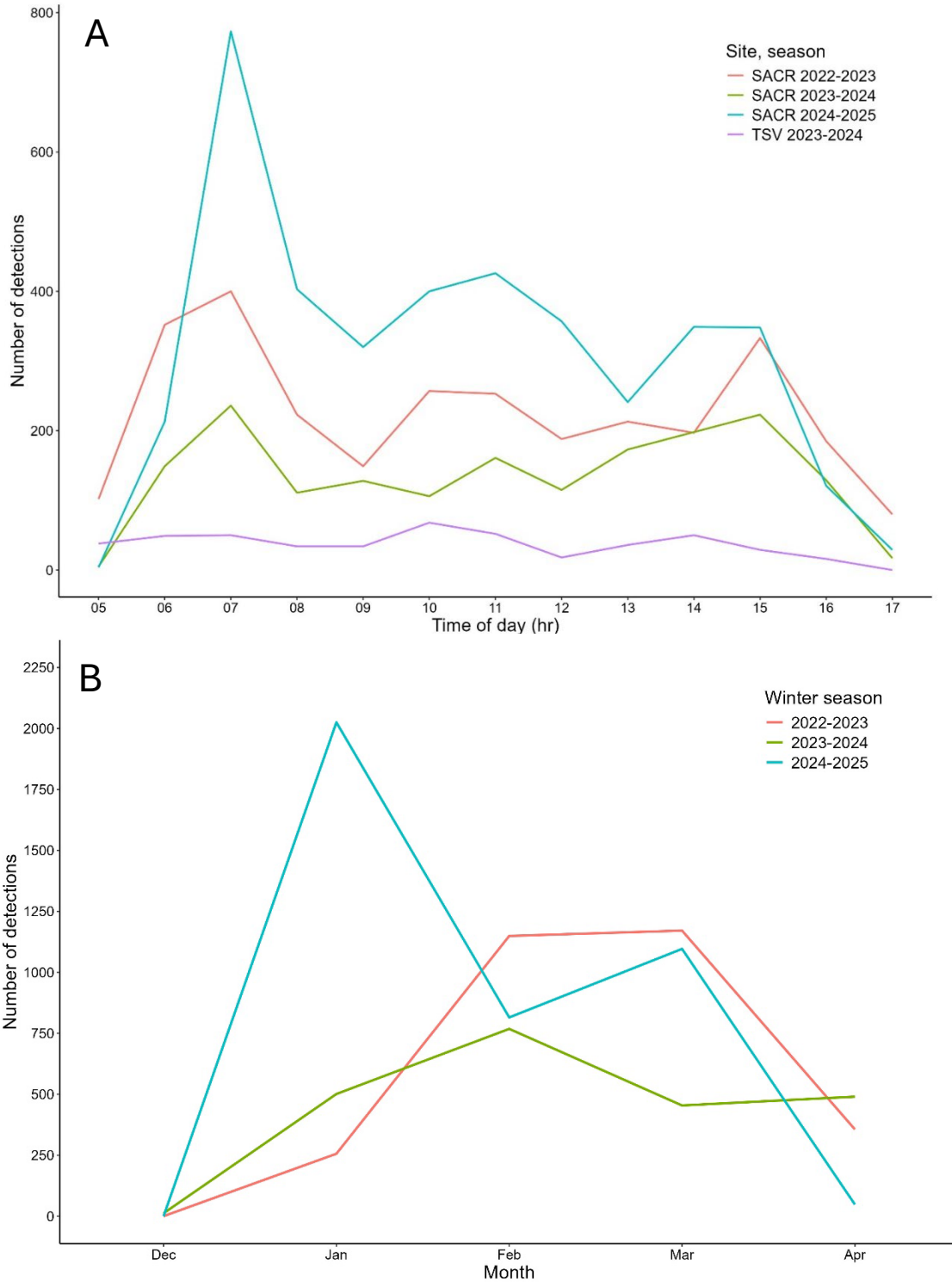


Figure 11. Temporal patterns of detections of RFID-tagged individuals by RFID-enabled feeders by (A) time of day (2400 hr) and (B) calendar month. Sandia Mountains (SACR) data were collected during the 2022–2023, 2023–2024, and 2024–2025 winter seasons; Taos Ski Valley (TSV) data were collected during the 2023–2024 season only. TSV detections in (B) are grouped together with SACR detections for 2023–2024 winter season.